Available online at www.sciencedirect.com
SCIENCE DIRECT
Polymer 46 (2005) 10045–10055
polymer
www.elsevier.com/locate/polymer

Controlled one-pot synthesis of pH-sensitive self-assembled diblock copolymers and their aggregation behavior

B.W. Mao[a], L.H. Gan[a,*], Y.Y. Gan[a], K.C. Tam[b], O.K. Tan[c]

[a]*Natural Sciences and Science Education, National Institute of Education, Nanyang Technological University, 1 Nanyang Walk, Singapore 637616, Singapore*
[b]*Singapore-MIT alliance, School of Mechanical and Aerospace Engineering, Nanyang Technological University, Singapore, Singapore*
[c]*School of Electrical and Electronic Engineering, Nanyang Technological University, Singapore, Singapore*

Received 20 April 2005; received in revised form 8 August 2005; accepted 16 August 2005
Available online 29 August 2005

Abstract

Diblock copolymers of *t*-butyl methacrylate (*t*BMA) and 2-(diethylamino)ethyl methacrylate (DEAEMA) were successfully synthesized by one-pot strategy via the atom transfer radical polymerization (ATRP). Kinetic results clearly demonstrated the controlled/'living' character of the polymerization. The zwitterionic block copolymers of poly(methacrylic acid-*b*-DEAEMA), obtained by hydrolysis of poly(*t*BMA-*b*-DEAEMA), showed pH-dependent reverse micellization behavior. Micellar aggregates formed from poly(MAA_{30}-*b*-$DEAEMA_{71}$), poly(MAA_{68}-*b*-$DEAEMA_{55}$) and poly(MAA_{64}-*b*-$DEAEMA_{44}$) had fairly low polydispersity index at both solutions of low pH of 2 and high pH of 12. Micelles formed at pH 2 were larger ($R_h \sim 40$–61 nm) with looser core due to hydration of the MAA. In the presence of simple electrolyte (0.3 mol dm^{-3} NaCl solution), the size of the micelles reduced by almost half while the aggregation number was little changed. This is attributed to the draining of the hydrated micellar core due to osmotic pressure. On the other hand, DEAEMA-core micelles formed at pH 12 were compact and much smaller ($R_h \sim 14$–22 nm). Addition of NaCl had only a small effect. The micellar size reduced only slightly due to the electrostatic screening effect and the aggregation number was almost unchanged.

Keywords: One-pot ATRP; Zwitterionic diblock copolymers; Kinetics

1. Introduction

Zwitterionic diblock copolymers with two water-soluble, oppositely charged polyelectrolytes blocks are an interesting class of polymeric materials which have attracted a great deal of interest in recent years because of their application as stabilizers, emulsifiers, dispersants [1–7], protein isolation and purification [8] and drug-delivery vehicles [9,10]. The copolymers aggregate into a variety of complex structures in aqueous solutions, depending on such factors as the block length ratio, solubility of the respective blocks, pH of the medium and salt effect. The association behavior of these molecules in solution is an important aspect for understanding its colloidal stability. Studies of aggregation behavior require the copolymers to have well-defined architecture so that the solution exhibits uniform physical properties. Well-defined diblock copolymers are usually synthesized by a variety of controlled/'living' polymerization methods among which are classical anionic polymerization, group transfer polymerization (GTP), reversible addition–fragmentation polymerization (RAFT) and atom transfer radical polymerization (ATRP).

More recently, another new class of pH-responsive zwitterionic diblock copolymer consisting blocks of weak base and weak acid have been synthesized and reported by us [11] and the Armes group [12,13]. These diblock copolymers self-assemble into micelles at low pH and the structure of the micelles is reversed at high pH. The association behavior of these pH-sensitive copolymers have been described as 'schizophrenic' by Armes et al. [12,13]. Typically the diblock copolymers are synthesized with tertiary amine methacrylates forming the weak basic blocks and carboxylic forming the weak acid blocks. Most of the early works have been focused on the diblock copolymers of 2-(dimethylamino)ethyl methacrylate (DMAEMA) and methacrylic acid (MAA). Creutz et al. [14–17] and Goloub

* Corresponding author. Tel.: +65 6790 3811; fax: +65 6896 9432.
E-mail address: lhgan@nie.edu.sg (L.H. Gan).

0032-3861/$ - see front matter © 2005 Elsevier Ltd. All rights reserved.
doi:10.1016/j.polymer.2005.08.048

et al. [18] have reported the synthesis of poly(DMAEMA-*b*-MAA) diblock copolymers by classical living anionic polymerization, whereas the diblock copolymer was synthesized by Armes et al. [19–21] using 2-tetrahydropyranyl methacrylate (THPMA) as a protected precursor utilizing group transfer polymerization (GTP). Donovan et al. [22] have prepared AB diblock copolymers based on DMAEMA and acrylic acid (AA) via RAFT. Other zwitterionic diblock copolymers such as poly[4-vinylbenzonic acid-*block*-2-*N*-(morpholino)ethyl methacrylate] (VBA-*b*-MEMA) [23] and poly[4-vinylbenzonic acid-*block*-2-(diethylamino)ethyl methacrylate] (VBA-*b*-DEAEMA) [12] have been synthesized via ATRP. The aggregation behavior of amphiphilic/zwitterionic block copolymers have been extensively studied by various groups which include those of Creutz et al. [14–16], Gohy et al. [17], Goloub et al. [18], Lowe and Armes [19,20], Bütün et al. [21], Matsumoto et al. [24], and Pispas and Hadjichristidis [25,26].

Until recently, most of the diblock copolymers synthesized by ATRP technique were prepared via a stepwise polymerization–isolation–polymerization approach. This approach requires the macroinitiator synthesized to be first separated and purified before the second monomer is introduced. Among the possible drawbacks of this approach is the partial loss of terminal functionality, leading to less than complete chain extension of the second block. The overall copolymer yields are generally poor. Liu et al. [27] first reported the one-pot synthesis of a ABC triblock copolymer via ATRP. Direct syntheses of zwitterionic diblock copolymers were recently reported by Li et al. [28], Bories-Azeau et al. [13], and Masci et al. [29]. Star polymers have also been successfully synthesized via one-pot ATRP [30].

We have recently reported the preliminary results on the synthesis of well-defined poly(MAA-*b*-DEAEMA) [11], through hydrolysis of poly(*t*BMA-*b*-DEAEMA) [31] synthesized via a step-by-step ATRP technique. As an extension of this work, we now report a convenient and well-controlled one-pot synthesis of poly(*t*BMA-*b*-DEAEMA) via ATRP with high yield and low polydispersity index (PDI). The pH-dependent aggregation behavior of poly(MAA-*b*-DEAEMA) in various pH are discussed.

2. Experimental

2.1. Materials

DEAEMA (98%, Merck) and *t*BMA (98%, Merck) were purified by passing through a basic alumina column and distilled prior to use. *p*-Toluenesulfonyl chloride (*p*-TsCl) (99%, Fluka), CuCl (99.99% Aldrich), 1,1,4,7,10,10-hexamethyl-triethylenetetramine (HMTETA) (97%, Aldrich), tetrahydrofuran (THF) (99.9%, Aldrich) and methanol (anhydrous 99.9%, Aldrich) were used as received. Milli-Q water was used for the preparation of all aqueous solutions.

2.2. Synthesis of block copolymer of tBMA and DEAEMA via one-pot ATRP

To a dry 25 ml Schlenk flask with a magnetic stirring bar, CuCl (0.0328 g, 0.332 mmol) was added and the Schlenk flask was evacuated and flushed with argon. Distilled *t*BMA (5.0 ml, 30.8 mmol), HMTETA (0.0903 ml, 0.332 mmol) and degassed methanol (2.5 ml) and distilled water (0.25 ml) were added to the Schlenk flask using degassed syringes and the mixture were stirred for 10 min. The mixture was degassed by three freeze–thaw cycles. Finally, *p*-TsCl (0.0633 g, 0.332 mmol) was added. The flask was then placed in a preheated oil bath maintained at 60 ± 0.2 °C. The *t*BMA polymerization was allowed to proceed with constant stirring. Aliquots were taken regularly for GPC analysis to assess the extent of polymerization. After 470 min, the reaction mixture became more viscous with ~90% of *t*BMA conversion as monitored by GPC. The second monomer, DEAEMA (2.7 ml, 13.4 mmol) was then added using a degassed syringe. The polymerization was carried out under the same conditions for 60 min. The polymerization was terminated by addition of 10 ml THF. The solution was passed through a basic alumina column and eluted with additional 100 ml of THF. After concentration using a rotary evaporator, the solution was poured into methanol/H_2O (1:1 v/v) mixture to precipitate the polymer. Final GPC results: $M_{n,tBMA}=13{,}000$, PDI = 1.13; $M_{n,diblock}=18{,}000$, PDI = 1.11.

2.3. Conversion of poly(tBMA-b-DEAEMA) to poly(MAA-b-DEAEMA)

The compositions of poly(*t*BMA-*b*-DEAEMA) copolymers could be quantified by ^{1}H NMR analysis. In CD_3OD, the chemical shift (δ in ppm) of the *t*-butyl group –$OC(CH_3)_3$, ($\delta=1.35$) of *t*BMA is well separated from those of the methylene groups –OCH_2– ($\delta=3.93$), –CH_2–CH_2–N< ($\delta=2.65$), and >N–CH_2CH_3 ($\delta=2.51$) of DEAEMA. The molar compositions of *t*BMA and DEAEMA of the copolymer can be calculated from the peak intensity ratio of the butyl group to the methylene groups of DEAEMA.

The *t*-butyl groups were hydrolyzed with concentrated hydrochloric acid in 1,4-dioxane under reflux for 8 h and the product was precipitated in *n*-hexane. The copolymer was washed with *n*-hexane four times and dried under vacuum. The FT-IR (KBr-pellet) spectrum showed a broad peak at 3500 cm^{-1}, corresponding to the absorption of –OH, indicating the formation of the carboxylic acid group. ^{1}H NMR analysis revealed that the hyhrolysis was nearly complete as no *t*-butyl groups were detected in the hydrolyzed sample.

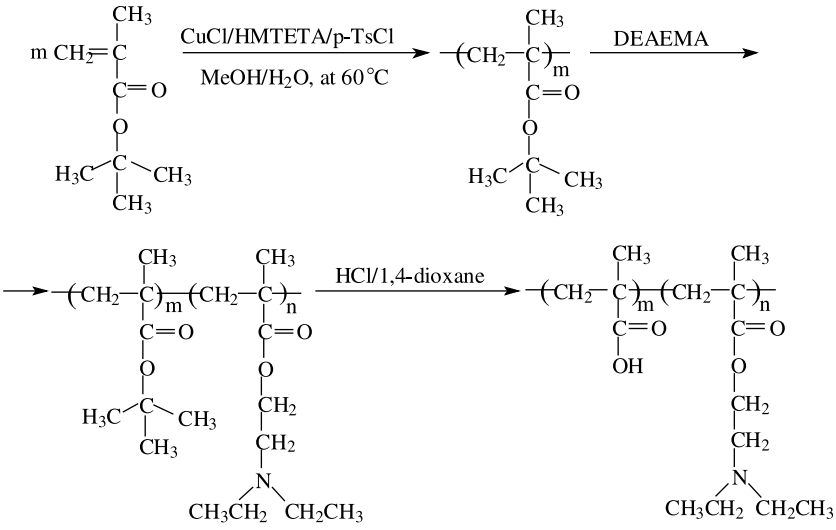

Scheme 1. One-pot synthesis of poly(*t*BMA-*b*-DEAEMA) and its hydrolysis to yield poly(MAA-*b*-DEAEMA).

2.4. Preparation of the block copolymer solution

A 0.1 wt% stock solution of each copolymer in water was prepared. This solution was further diluted to 0.01 wt% in glass vessels.

2.5. Characterization

M_n and M_w/M_n (PDI) of the polymers were determined by gel permeation chromatography (GPC). An Agilent 1100 series GPC system equipped with a LC pump, PLgel 5 μm MIXED-C column and RI detector was used. The column was calibrated with narrow molecular weight polystyrene standards. HPLC grade THF stabilized with 2,6-*tert*-butyl-4-methylphenol (BHT) containing 1% triethylamine was used as a mobile phase, at a flow rate of 1.0 ml min^{-1}. ^1H NMR spectra were recorded using a Bruker DRX400 spectrometer in $CDCl_3$. For polymers prepared using the *p*-TsCl initiator, ^1H NMR spectra show distinctive peaks for the phenyl group [$\delta = 7.3$–7.4 (2H); 7.7–7.8 (2H)] and the repeat units. Absolute M_n values could be obtained from the integral ratios of the phenyl group to the relevant peaks of the monomer units (i.e. *t*-butyl group for *t*BMA and the methylene group –OCH_2CH_2– for DEAEMA).

2.6. Potentiometric titration

An ABU93 Triburet titration system equipped with radiometer pHG201 pH glass and radiometer REF201 reference electrode was used to conduct the potentiometric titrations. All the titrations were performed under constant stirring in a titration vessel filled with 100 ml of 0.04 wt% polymer solution at 25 °C. Standard NaOH solution (1 M) (from Merck) was used, and a lag time of 1 min was allowed between two dosages to ensure that the reaction has reached equilibrium.

2.6.1. Static light scattering

Static light scattering (SLS) was used to measure and analyze the time-averaged scattered intensities. The method is often used to determine microscopic properties of particles such as the *z*-average radius of gyration (R_g), the weight-average molecular weight (M_w), and the second virial coefficient (A_2) according to Eq. (1):

$$\frac{KC}{R_\theta} = \frac{1}{M_w}\left[1 + \frac{16\pi^2 n^2 \langle R_g^2\rangle \sin^2(\theta/2)}{3\lambda^2}\right] + 2A_2C \qquad (1)$$

where, the Rayleigh ratio, $R_\theta = (I_s r^2/I_i \sin\theta)$; $K = [4\pi^2 n^2 (\partial n/\partial C)^2/(N_A\lambda^4)]$; C is the concentration of the polymer solution; n is the refractive index of the solvent; θ is the angle of measurement; λ is the wavelength of laser light; N_A is Avogadro's constant; and $(\partial n/\partial C)$ is the refractive index increment of the polymer solution. A plot of (KC/R_θ) versus $[\sin^2(\theta/2) + kC]$ (where k is an arbitrary constant) can be used to determine the molecular parameters. By extrapolating the data to zero angles and concentrations, R_g and A_2 can be obtained from the slopes, respectively. A simultaneous extrapolation to zero angle and concentration yields an intercept, which is the inverse of the M_w.

2.6.2. Dynamic light scattering

The frequency of scattered light fluctuates around the incident light due to the constant motion of the polymer molecules. Dynamic light scattering (DLS) measures the intensity fluctuations with time and correlates these fluctuations with the properties of the scattering objects. In general, the terms of correlation functions of dynamic variables are always used to describe the response of the scattering molecules to the incident light. The translational diffusion coefficients, D, can be determined by Eq. (2), where Γ is the decay rate, which is the inverse of the relaxation time (τ); q is the scattering vector ($q = 4\pi n \sin(\theta/2)/\lambda$), where θ is the scattering angle, n is the refractive

Table 1
Table1 One-pot synthesis of poly(*t*BMA-*b*-DEAEMA) at 60 °C

Sample	M_n	M_w/M_n	*t*BMA/DEAEMA	
			By GPC	By ^{1}H NMR
Poly(tBMA$_{30}$-*b*-DEAEMA$_{71}$)	17,500	1.12	0.44	0.42
Poly(tBMA$_{68}$-*b*-DEAEMA$_{55}$)	20,000	1.13	1.27	1.24
Poly(tBMA$_{64}$-*b*-DEAEMA$_{44}$)	18,000	1.11	1.49	1.45

$[CuCl]_0=[HMTETA]_0=[p\text{-}TsCl]_0=0.332$ mmol; in the mixture of methanol and H_2O (volume ratio, 10:1) at 60 °C.

index of the solution, and λ is the wavelength of the incident light.

$$\Gamma = Dq^2 \quad (2)$$

The diffusion coefficient at infinite dilution (D_0) for spherical particles is related to the hydrodynamic radius R_h by the Stokes–Einstein equation (Eq. (3)):

$$R_h = kT/6\pi\eta D_0 \quad (3)$$

where k is the Boltzmann constant; T is the absolute temperature; and η is the viscosity of the solvent. The values of R_h were calculated by assuming $D \approx D_0$ for dilute solutions.

A Brookhaven BIS200 laser scattering system was used to perform the static and dynamic light scattering experiments. The light source is a power-adjustable vertically polarized 350 mW argon ion laser with a wavelength of 488 nm. The inverse Laplace transform of

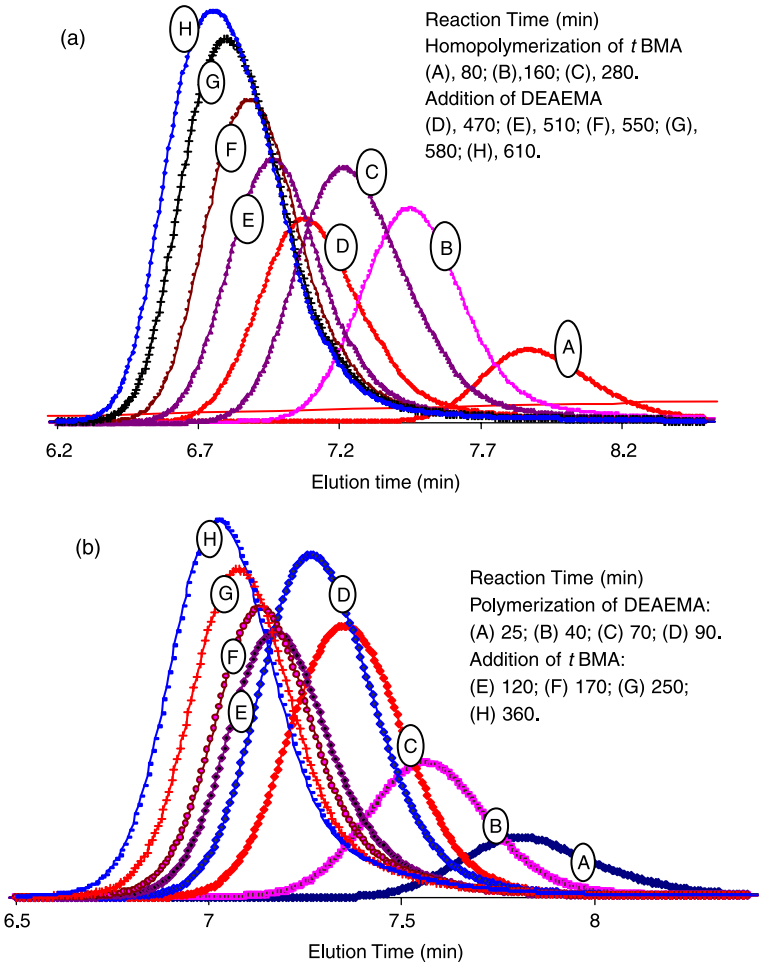

Fig. 1. GPC traces of block copolymer DEAEMA and *t*BMA prepared in one pot in methanol/H_2O mixture (v/v 10:1) at 60 °C. $[CuCl]_0=[HMTETA]_0=[p\text{-}TsCl]_0=0.332$ mmol. (a) *t*BMA polymerization is from A to D; copolymerization with DEAEMA is from D to H; $[tBMA]_0=30.8$ mmol; $[DEAEMA]_0=33.3$ mmol. (b) DEAEMA polymerization is from A to D; copolymerization with DEAEMA is from E to H; $[DEAEMA]_0=24.9$ mmol; $[tBMA]_0=16.6$ mmol.

REPES supplied with the GENDIST software package was used to analyze the time correlation function (TCF), and the probability of reject was set to 0.5.

3. Results and discussion

3.1. One-pot synthesis of poly(tBMA-b-DEAEMA) in protic medium

The one-pot synthesis route of poly(*t*BMA-*b*-DEAEMA) and its hydrolysis to poly(MAA-*b*-DEAEMA) are outlined in Scheme 1.

Homopolymerization of *t*BMA was first performed to high conversion (>90%), after which the second DEAEMA monomer was added. The composition of three poly(*t*BMA-*b*-DEAEMA) samples of different block lengths are presented in Table 1.

The progress of polymerization was monitored by GPC. The GPC traces as a function of reaction time for poly(*t*BMA-*b*-DEAEMA) show a smooth increase in molar masses (Fig. 1(a)). All the GPC traces, including those after the introduction of the second monomer are symmetrical, indicating good extension of the second block. The increase in molar mass (M_n) and change in PDI as a function of reaction time are shown in Fig. 2(a). The rate of polymerization of DEAEMA for the formation of second block (stage II) is clearly faster than that of the *t*BMA forming the first block (stage I). The PDI decreases with longer polymerization time as is expected for controlled ATRP.

The results from the kinetic study confirmed the polymerization was indeed under controlled/'living' conditions throughout the reaction. The first-order kinetic plots of $\ln([M_0]/[M])$ versus time are linear (Fig. 3(a)), in accordance with the following equation for living polymerizations proposed by Matyjaszewski et al. [32]

$$\ln\left(\frac{[M]_0}{[M]}\right) = k_p K_{eq} \frac{[RX][Cu(I)]}{[Cu(II)]} t = k_{app} t$$

As the architecture of the second block could be affected

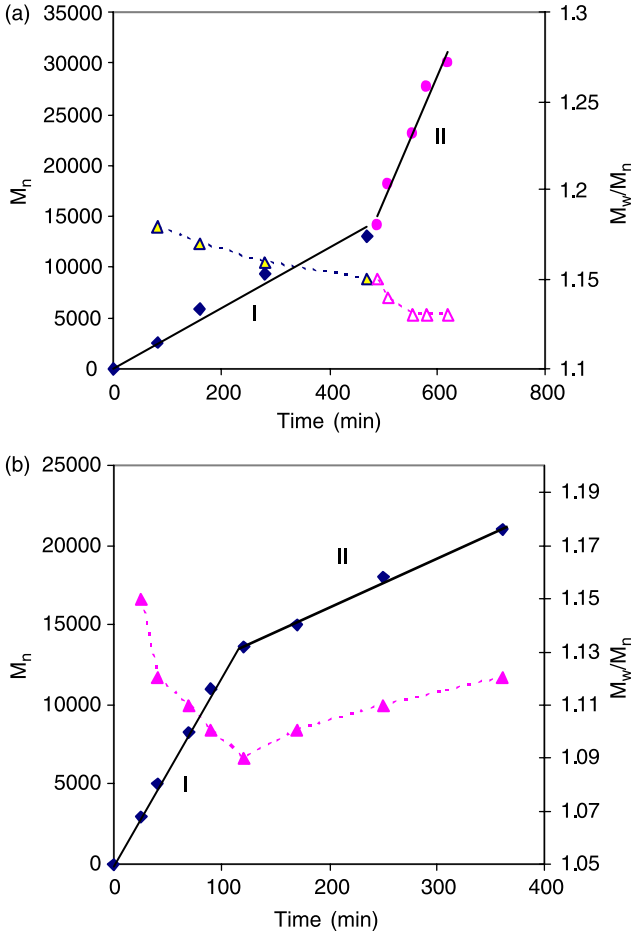

Fig. 2. Plots of M_n and PDI for block copolymer *t*BMA and DEAEMA as a function of reaction time. Reaction conditions: $[CuCl]_0=[HMTETA]_0=[p\text{-}TsCl]_0=0.332$ mmol; in methanol/H_2O mixture (v/v 10:1) at 60 °C. (a) (I): *t*BMA; $[tBMA]_0=30.8$ mmol; $[DEAEMA]_0=24.9$ mmol; (b) (I): DEAEMA; $[DEAEMA]_0=24.9$ mmol; $[tBMA]_0=16.6$ mmol.

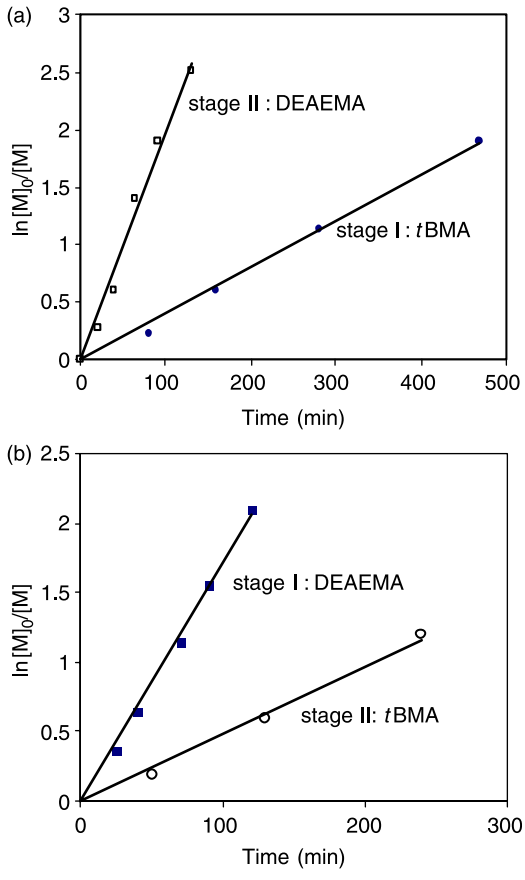

Fig. 3. Semilogarithmic kinetic plots for ATRP of block copolymer DEAEMA and *t*BMA in methanol/H_2O mixture (v/v 10:1) at 60 °C. $[CuCl]_0=[HMTETA]_0=[p\text{-}TsCl]_0=0.332$ mmol; (a) stage I, polymerization *t*BMA; (b) stage I, polymerization DEAEMA; experimental conditions: (a) $[tBMA]_0=30.8$ mmol; $[DEAEMA]_0=24.9$ mmol; (b) $[tBMA]_0=16.6$ mmol; $[DEAEMA]_0=24.9$ mmol.

Table 2
Apparent rate constant k_{app} for the homopolymerization and copolymerization

Polymer	k_{app} (min^{-1})
Poly(*t*BMA)	0.0045
Poly(DEAEMA-*b*-*t*BMA)[a]	0.0049
Poly(DEAEMA)	0.0171
Poly(*t*BMA-*b*-DEAEMA)[a]	0.0198

[a] For block copolymers, k_{app} refers to the polymerization of second block.

by the relative rates of polymerization of the two monomers, another set of experiments, where DEAEMA was polymerized first, followed by copolymerization with *t*BMA was performed. It was found that this reverse copolymerization process was almost equally well-controlled, as shown in the corresponding Figs. 1(b) and 3(b). The apparent first-order rate constant, k_{app}, for the second block under the copolymerization conditions agrees well with the respective homopolymerization rate constants of *t*BMA and DEAEMA (Table 2). Henceforth, the kinetics of the chain extension of the second block using macroinitiator was not affected under the experimental conditions. The results also indicate that the second block was formed with minimal random copolymerization of the first monomer. This is reasonable because (i) the apparent rate constant for the polymerization of DEAEMA is greater than that of *t*BMA with k_{app}(DEAEMA) ~ 3.5 k_{app}(*t*BMA) and (ii) [DEAEMA] ≫ [*t*BMA] for most of the time during the copolymerization as only residual *t*BMA was present. It was found that even in the reverse order of copolymerization forming poly(DEAEMA-*b*-*t*BMA), good extension of the second block was also obtained, judging by the kinetic data. Nevertheless, it should be noted that the kinetic data may not be sensitive enough to reveal the expected rate change caused by the incorporation of a small amount of the second monomer.

Based on the above consideration, only poly(*t*BMA-*b*-DEAEMA) were used for the aggregation studies, as these copolymers are likely to have better defined block junction compared to poly(DEAEMA-*b*-*t*BMA). Indeed, poly(MAA-*b*-DEAEMA), derived from poly(*t*BMA-*b*-DEAEMA) formed low polydispersity micellar aggregates (see later results).

3.2. Aggregation studies

The morphologies of aggregates formed by zwitterionic diblock copolymers in water have been widely studied. In most cases, spherical aggregates of core–shell structures are formed, where the core is formed by the insoluble blocks and the surrounding shell is formed by the solvated blocks. However, more complicated structures (i.e. compound micelles) are also observed for some diblock copolymers, due to various factors such as hydrophile–lypophile balance (HLB), ratio of the block lengths and perfect/imperfect block architectures. Samples with less well-defined block structures are expected to result in more complex aggregation behaviors in solution. In our previous communication of the pH-responsive 'schizophrenic' micellization of poly(MAA-*b*-DEAEMA), the diblock copolymer was synthesized by protecting group chemistry via a polymerization–isolation–polymerization ATRP process [11]. In aqueous solution, at low pH (< ~4), spherical micelles comprised the undissociated MAA forming the hydrophobic core surrounded by the protonated DEAEMA shell. At high pH (> ~9), reverse micelles containing the deprotonated hydrophobic DEAEMA core and hydrophilic corona shell were formed. At around the isoelectric point (IEP), at which the positive and negative charges are equal, precipitation of the copolymer occurs, as shown in Scheme 2.

We have reexamined the micellization behavior of poly(MAA-*b*-DEAEMA), using the well-defined copolymers obtained by the one-pot synthesis described above.

3.3. Titration: pH and conductivity measurements

In the titration studies, both the conductivity and pH were measured simultaneously. The conducting species in the polymer solution are H^+, Na^+, OH^-, Cl^-, and the macroion (*p*). Hence the conductivity can be expressed by Eq. (4).

$$\Lambda = C_{Na^+}\lambda_{Na^+} + C_{H^+}\lambda_{H^+} + C_{OH^-}\lambda_{OH^-} + C_{Cl^-}\lambda_{Cl^-} + C_P\lambda_P \quad (4)$$

where C_i is the concentration of free ion in solution, and λ_i is the molar conductivity of the corresponding ion. Representative titration curves of poly(MAA_{68}-*b*-$DEAEMA_{55}$)

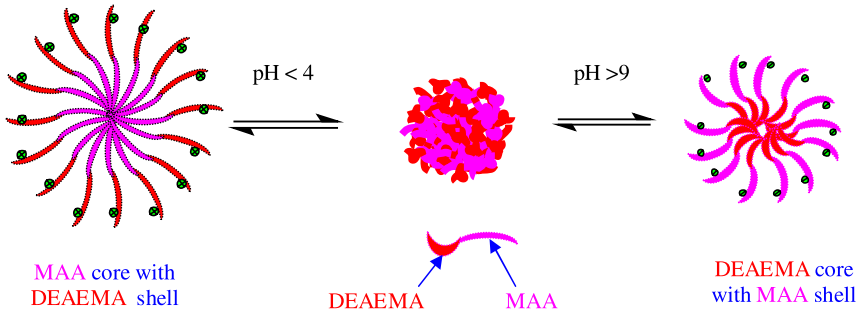

Scheme 2. The pH-dependent reversible micellization exhibited by poly(MAA-*b*-DEAEMA).

Table 3
Calculated and observed conductivities at the two inflexion points A and B

Polymer solution	pH	NaOH (mmol)	Conductivity (Λ) (ms/cm)	
			$\Lambda_{caculated}$	$\Lambda_{observed}$
Poly(MAA_{30}-*b*-$DEAEMA_{71}$) 0.0404 g in 100 ml H_2O *n*(DEAEMA)=1.	4.73	0.05	138	128
39×10^{-4} mol *n*(MAA)=0.58×10^{-4} mol	10.18	0.18	227	228
Poly(MAA_{68}-*b*-$DEAEMA_{55}$) 0.0330 g in 100 ml H_2O *n*(DEAEMA)=0.	5.06	0.07	109	101
92×10^{-4} mol *n*(MAA)=1.13×10^{-4} mol	9.91	0.19	192	177
Poly(MAA_{64}-*b*-$DEAEMA_{44}$) 0.0405 g in 100 ml H_2O *n*(DEAEMA)=1.	4.25	1.1	162	127
15×10^{-4} mol n(MAA)=1.688×10^{-4} mol	9.79	2.7	235	209

are shown in Fig. 4. During the titration, the concentrations of all the conducting species change except that of Cl^- ion, which remains unchanged throughout. The conductivity curve consists of three distinct regions with different slopes. The initial conductivity of the polymer solution consists of the conductivity of free H^+ ions ($\lambda_{H^+} = 350$ S cm^2 mol^{-1} at 25 °C), free Cl^- ($\lambda_{Cl^-} = 76.3$ S cm^2 mol^{-1} at 25 °C) and the protonated DEAEMA macroions. Addition of NaOH reduces the concentrations of H^+ and protonated DEAEMA, while the concentration of Na^+ increases. In the first stage of titration, a decrease in conductivity was observed due to the decrease of [H^+]. This is offset by the increase in conductivity due to increasing [Na^+] ($\lambda_{Na^+} = 50.5$ S cm^2 mol^{-1} at 25 °C) as more NaOH is added. A turning point is reached at A, where $\Lambda = 109$ S cm^2 mol^{-1} at pH 5.06, from where a gradual increase of conductivity is observed. Deprotonation of DEAEMA and ionization of the MAA carboxylic acid groups continue with further addition of NaOH, which is accompanied by increasing conductivity and pH. Another change of slope in the conductivity curve is observed after reaching point B. From point B, the conductivity increases sharply, signifying that ionization of the MAA block is complete.

The amount of NaOH (0.19 mmol) added at point B agree reasonably well with the combined quantities of DEAEMA HCl (0.92×10^{-4} mol) and MAA (1.13×10^{-4} mol) in the

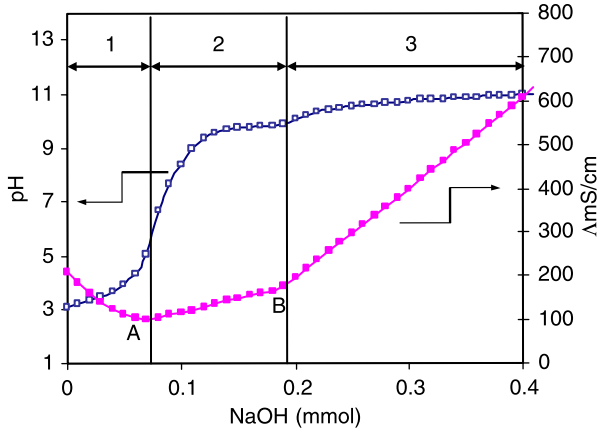

Fig. 4. Titration curves [pH (□) and conductivity (■)] of solution of 0.0330 g poly(MAA_{68}-*b*-$DEAEMA_{55}$) in 100 ml H_2O.

copolymer. Assuming that the counterion binding of the macroions is negligible and neglecting the contribution from the macroions, the conductivity of the solution at the two inflexion points A and B can be calculated from the concentrations and molar conductance values of the free ions. The theoretical values for the three polymer solutions compare reasonably well with those observed (Table 3).

These results suggest that micelles comprising hydrophobic MAA cores and protonated DEAEMA corona shells are formed below point A. On increasing the pH beyond point A, the carboxylic acid groups of MAA segment become progressively ionized. The $-COO^-$ groups interact with protonated DEAEMA residues through electrostatic attraction, and precipitation of the copolymer is observed at pH ~ 5. As the pH increases beyond the IEP, the DEAEMA block is progressively deprotonated, and the electrostatic balance is destroyed. The cloudy solution turns clear again due to the formation of reverse micelles containing deprotonated hydrophobic DEAEMA cores and anionic MAA corona shells.

3.4. UV–vis spectrophotometry and isoelectric point

The % transmittance (%*T*) of aqueous copolymer solutions at different pH were measured at a fixed wavelength of 488 nm. All three copolymers were completely soluble in solutions at pH < ~4 and pH > ~9, but precipitation occurs at their respective IEPs. The %*T* versus pH curves revealed insolubility over a range of pH, due to the attractive electrostatic interactions between the polymer chains (Fig. 5). Thus, the IEP was not clearly defined from the %*T* data. However, the pH range of insolubility shifts towards lower pH with increasing MAA:DEAEMA molar ratio and the range increases from 0.42 for poly(MAA_{30}-*b*-$DEAEMA_{71}$), to 1.25 for poly(MAA_{68}-*b*-$DEAEMA_{55}$) and to 1.45 for poly(MAA_{64}-*b*-$DEAEMA_{44}$). Interestingly, the pH range of insolubility for poly(MAA_{30}-*b*-$DEAEMA_{71}$) is much narrower, possibly due to its highly asymmetric block composition. As an approximation, the IEP is taken as the midpoint of the pH range of precipitation [17]. The results are presented in Table 4, showing the observed IEP values are in good agreement with those calculated using the equation reported by Patrickios et al. [33]

Table 4
Calculated and observed IEP values of the three poly(MAA-*b*-DEAEMA) diblock copolymers

Copolymer	Observed IEP	Calculated IEP
Poly(MAA_{30}-*b*-$DEAEMA_{71}$)	7.42	7.22
Poly(MAA_{68}-*b*-$DEAEMA_{55}$)	6.62	6.38
Poly(MAA_{64}-*b*-$DEAEMA_{44}$)	6.35	6.12

$$pI = pK_b + \log\{[(1-R)/R + [((1-R)/R)^2 + (4/R)10^{pK_a - pK_b}]^{1/2}]/2\}$$

where, R, the molar ratio of the acid to base, and pK_a and pK_b, the dissociation constants of the negative and positive charges.

3.5. Laser light scattering

The dynamic light scattering (DLS) data obtained from the present studies revealed only single translational diffusion mode in the decay time distribution function for polymer solutions at pH 2 and pH 12. The single translational mode corresponds to the formation of micelles. No small aggregates were detected for all the three copolymers, as the result of their well-defined block architectures.

Representative DLS results for poly(MAA_{68}-*b*-$DEAEMA_{55}$) solutions at pH 12 are presented in Fig. 6. The decay time distribution functions measured at 90° yielded one single and almost identical peak for solutions of different concentrations (Fig. 6(a)), indicating that the micellar structures were concentration-independent. When measured at increasing angles, the peak relaxation time shifted towards lower values (Fig. 6(b)), confirming that only one type of particle was present. The relaxation rate Γ (the reciprocal of peak relaxation time) was found to be proportional to the square of the scattering vector (q^2), confirming that the scattering objects were related to translational diffusion.

The scattering intensity for the average hydrodynamic diameter (D_h) measured at 90° of a 0.02 wt% aqueous solution of poly(MAA_{68}-*b*-$DEAEMA_{55}$) is shown in Fig. 7. At pH 12, core–shell micelles are formed. The polydispersity of the size of micelles, evaluated through the ratio μ_2/Γ^2 by cumulants analysis [26,34], where μ_2 is the second moment in the cumulant expansion of the correlation function and Γ is the decay rate, is small with a value of 0.099. The average hydrodynamic diameter of the particles is 44 nm. At pH 2, the MAA-core micelles formed are much larger (D_h = 122 nm) though the polydispersity is still low at 0.115. This suggests that the size distribution of the micelles is much narrower at high pH aqueous solution than those formed at low pH aqueous solution. Apparently, the MAA blocks form much looser micelle cores due to hydration, which is confirmed by the study of salt effect (see below).

Static light scattering (SLS) studies were also performed.

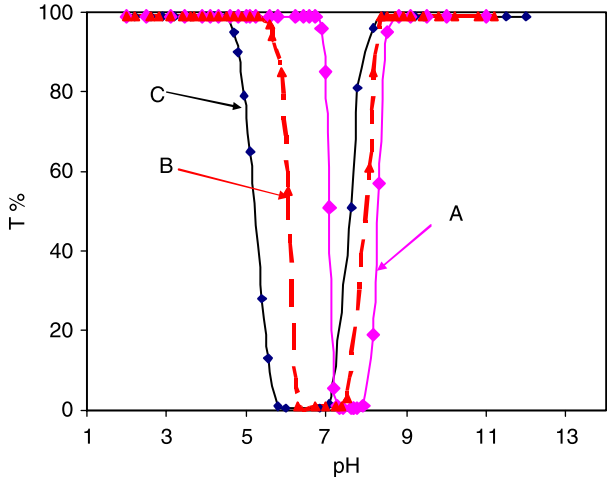

Fig. 5. %T of 0.04 wt% copolymer aqueous solutions at different pH. A, poly(MAA_{30}-*b*-$DEAEMA_{71}$); B, poly(MAA_{68}-*b*-$DEAEMA_{55}$) and C, poly(MAA_{64}-*b*-$DEAEMA_{44}$).

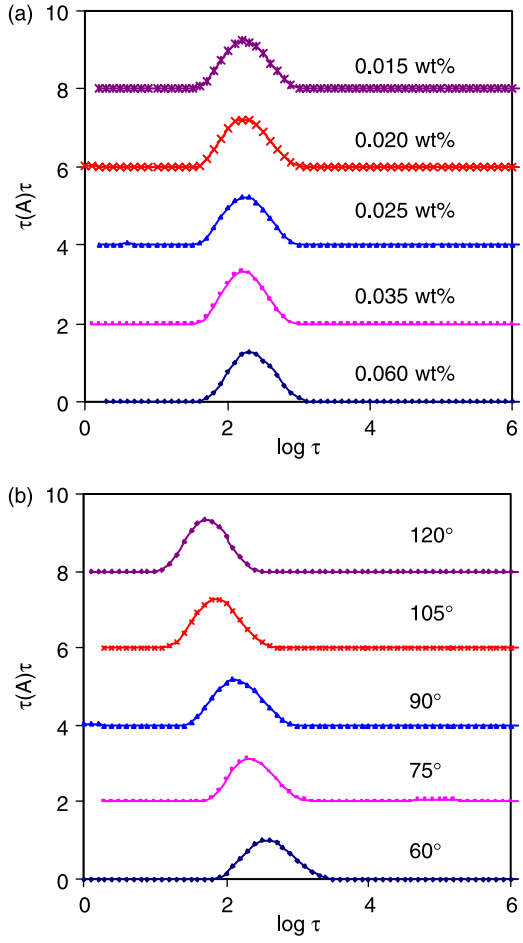

Fig. 6. Decay time distribution functions for the poly(MAA_{68}-*b*-$DEAEMA_{55}$) in aqueous solution (pH = 12) at 25 °C: (a) measured at angle 90° with different concentration. (b) 0.02 wt% polymer solution at different measurement angles.

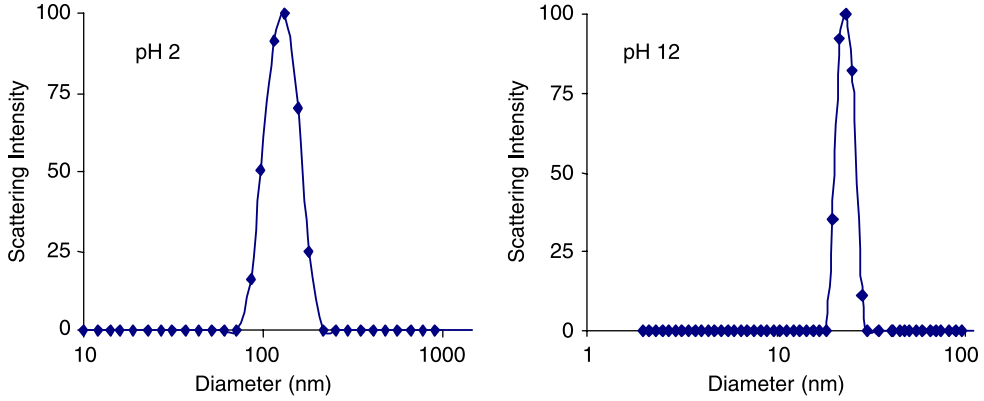

Fig. 7. Average hydrodynamic diameter (D_h) and scattering intensity (at 90°) of 0.02 wt% aqueous solution of poly(MAA_{68}-*b*-$DEAEMA_{55}$) at pH 2 and pH 12.

A typical Zimm plot of poly(MAA_{68}-*b*-$DEAEMA_{55}$) aqueous solution at pH 2 is shown in Fig. 8. The weight-average micelle masses ($M_{w,micelles}$), and micelle aggregation numbers ($N_{aggregation}$) were calculated. Furthermore, using $\rho = M_w/[4\pi(R_h)^3/3]$, where R_h is the hydrodynamic radius, the average densities (ρ) of the micelles were also estimated. The results are summarized in Table 5. All three poly(MAA-*b*-DEAEMA) copolymers show similar aggregation behaviors. The MAA-core micelles formed at low pH are relatively large with greater aggregation numbers, whereas the DEAEMA-core micelles are much more compact, with much smaller R_h. Consequently, the average densities of DEAEMA-core micelles are much higher than those of the MAA-core micelles.

3.5.1. Salt effect

It was found that addition of a simple salt, NaCl, greatly reduced the size of the aggregates at low pH, but had an insignificant effect at high pH. The changes in R_h as a function of [NaCl] at pH 2 and pH 12 are shown in Fig. 9. At pH 2, the R_h decreases rapidly in 0.1 mol dm^{-3} NaCl solution and its value is reduced almost by half at 0.2 mol dm^{-3} NaCl. The size remains little changed at higher NaCl concentrations. The effect of salt is due (i) to the screening of the electrostatic repulsions within the charged micelle corona, and, more importantly, (ii) to draining of the hydrated MAA cores because of the osmotic effect. Conversely, the much more compact DEAEMA cores are hardly affected by the addition of NaCl. The aggregation parameters for the copolymers in 0.3 mol dm^{-3} NaCl are presented in Table 6. It is noted that the ratios of R_g/R_h had become smaller, both at pH 2 and pH 12, suggesting the micelles are more compact in the presence of NaCl due to the osmotic effect.

4. Conclusions

Well-defined zwitterionic block copolymers based on *t*BMA and DEAEMA were successfully synthesized by

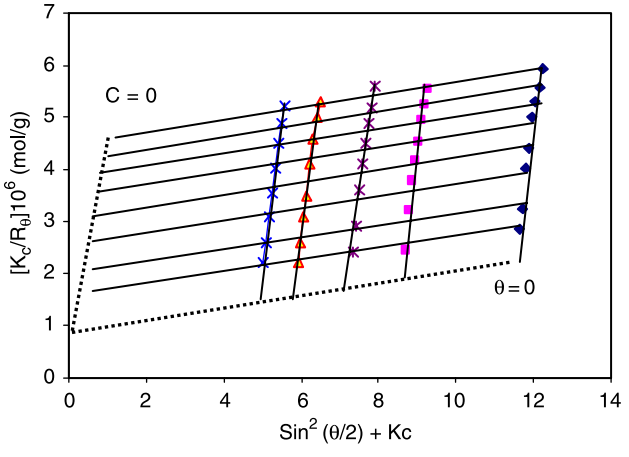

Fig. 8. Zimm plot of aggregations formed from poly(MAA_{68}-*b*-$DEAEMA_{55}$) in aqueous solution at pH 2 at room temperature. The concentrations (mg/ml) were: 0.32, 0.39, 0.53, 0.77, 1.26; and the scattering angles (°) were: 30, 45, 60, 75, 90, 105, 120, 135.

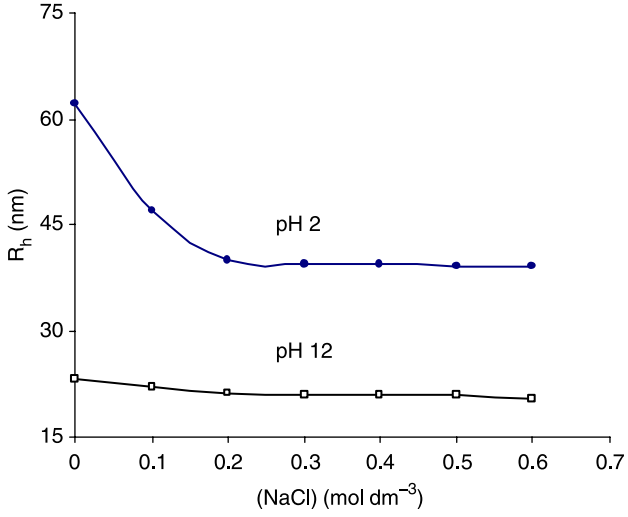

Fig. 9. The micelle hydrodynamic radius (R_h) of poly(MAA_{68}-*b*-$DEAEMA_{55}$) aqueous solution (0.02 wt%) as a function of NaCl concentration.

Table 5
Static and dynamic light scattering data obtained for the two reverse micelles formed by poly(MAA-*b*-DEAEMA) in aqueous solution at 25 °C

	MAA-core micelles at pH 2			DEAEMA-core micelles at pH 12		
	A	B	C	A	B	C
d*n*/d*c*	0.162	0.166	0.164	0.168	0.169	0.167
$M_{w,micelles}$(aggregates)	2.00×10^6	3.2×10^6	2.5×10^6	8.4×10^5	1.1×10^6	7.3×10^5
R_g (nm)	42.8	61.1	50.2	18.4	23.0	13.6
R_h (nm)	40.5	60.9	52.5	18.0	22.2	14.1
R_g/R_h	1.06	1.01	0.96	1.02	1.03	0.97
$N_{aggregation}$[a]	124	200	156	54	68	53
Polydispersity	0.103	0.115	0.112	0.093	0.099	0.101
ρ (g cm^{-3})	0.012	0.006	0.007	0.055	0.038	0.099

A, poly(MAA_{30}-*b*-$DEAEMA_{71}$); B, poly(MAA_{68}-*b*-$DEAEMA_{55}$); C, poly(MAA_{64}-*b*-$DEAEMA_{44}$).
[a] $N_{aggregation}=M_w$(aggregates)/M_w(polymer).

Table 6
Light scattering data of poly(MAA-*b*-DEAEMA) aqueous solutions in the present of 0.3 mol dm^{-3} NaCl at 25 °C

Conditions	MAA-core micelles at pH 2			DEAEMA-core micelles at pH 12		
	A	B	C	A	B	C
$M_{w,micelles}$ (aggregates)	1.80×10^6	3.1×10^6	2.4×10^6	8.3×10^5	10×10^5	6.9×10^5
R_g (nm)	29.7	39.3	32.1	14.2	18.7	11.9
R_h (nm)	31.2	41.9	34.2	15.6	19.8	12.6
R_g/R_h	0.95	0.93	0.93	0.91	0.94	0.94
$N_{aggregation}$[a]	120	195	149	52	62	50
Polydispersity	0.093	0.085	0.088	0.091	0.092	0.090
ρ (g cm^{-3})	0.023	0.016	0.023	0.084	0.049	0.132

A, poly(MAA_{30}-*b*-$DEAEMA_{71}$); B, poly(MAA_{68}-*b*-$DEAEMA_{55}$); C, poly(MAA_{64}-*b*-$DEAEMA_{44}$). Note: It was found that d*n*/d*c* values were roughly the same for the copolymer solutions with and without salt.
[a] $N_{aggregation}=M_w$(aggregates)/M_w(polymer).

one-pot approach via ATRP. This synthesis approach produced copolymers in high yield, and more importantly with well-defined block architectures. Kinetic studies revealed that the second stage block polymerization was as efficient as the first stage homopolymerization. In order to achieve high purity of the second block, it is important that the monomer with the faster polymerization rate should be used for the second block so as to minimize undesirable random copolymerization. All three copolymers, poly(MAA_{30}-*b*-$DEAEMA_{71}$), poly(MAA_{68}-*b*-$DEAEMA_{55}$) and poly(MAA_{64}-*b*-$DEAEMA_{44}$) formed micellar aggregates with low polydispersity indices, indicating well-defined block architectures. The block copolymers exhibit reversible micellization behavior at different pH. The precipitation range around the IEP varies for different copolymers, depending on their block compositions.

Acknowledgements

This research was funded by the academic fund, National Institute of Education (NIE), Nanyang Technological University, RP15/00GLH. MBW thanks NIE for the postgraduate research scholarship.

References

[1] Price C. In: Goodman I, editor. Developments in block copolymers-1. London: Applied Science Publishers; 1982.
[2] Selb J, Callot YD. In: Goodman I, editor. Developments in block copolymers-2. London: Applied Science Publishers; 1986.
[3] Baines FL, Armes SP, Billingham NC, Tuzar Z. Macromolecules 1996;29:8151.
[4] Baines FL, Dionisio S, Billingham NC, Armes SP. Macromolecules 1996;29:3096.
[5] Beadle PM, Rowan L, Mykytituk J, Billingham NC, Armes SP. Polymer 1993;34:1561.
[6] De Laat AWM, Derks WPT. Colloids Surf A: Physicochem Eng Aspects 1993;71:147.
[7] Hamley IW. The physics of block copolymers. Oxford, UK: Oxford University Press; 1999.
[8] Patrickios CS, Yamasaki EN. Anal Biochem 1995;231:82.
[9] Qiu Y, Park K. Adv Drug Deliv Rev 2001;53:321.
[10] Torchilin VP. J Controlled Release 2001;73:137.
[11] Dai S, Ravi P, Tam KC, Mao BW, Gan LH. Langmuir 2003;19:5175.
[12] Liu S, Armes SP. Angew Chem Int Ed 2002;41:1413.
[13] Bories-Azeau X, Armes SP, van den Haak HJW. Macromolecules 2004;37:2348.
[14] Creutz S, van Stam J, Antoun S, De Schryver FC, Jérôme R. Macromolecules 1997;30:4078.
[15] Creutz S, Teyssié P, Jérôme R. Macromolecules 1997;30:6.
[16] Creutz S, van Stam J, De Schryver FC, Jérôme R. Macromolecules 1998;31:681.
[17] Gohy JF, Creutz S, Garcia M, Mahltig B, Stamm M, Jérôme R. Macromolecules 2000;33:6378.

[18] Goloub T, de Keizer A, Cohen Stuart MA. Macromolecules 1999;32:8441.
[19] Lowe AB, Billingham NC, Armes SP. Chem Commun 1997;1035.
[20] Lowe AB, Billingham NC, Armes SP. Macromolecules 1998;31:5991.
[21] Bütün V, Lowe AB, Billingham NC, Armes SP. J Am Chem Soc 1999;121:4288.
[22] Donovan MS, Lowe AB, McCormick CL. ACS Polym Prepr 1999;40(2):281.
[23] Liu S, Armes SP. Langmuir 2003;19:4432.
[24] Matsumoto K, Kubota M, Matsuoka H, Yamaoka H. Macromolecules 1999;32:4464.
[25] Pispas S, Hadjichristidis N. Langmuir 2003;19:48.
[26] Pispas S, Hadjichristidis N. Macromolecules 2003;36:8732.
[27] Liu S, Armes SP. J Am Chem Soc 2001;123:9910.
[28] Li Y, Armes SP, Jin X, Zhu S. Macromolecules 2003;36:8268.
[29] Masci G, Bontempo D, Tiso N, Diociaiuti M, Mannina L, Capitani D, et al. Macromolecules 2004;37:4464.
[30] Deng G, Chen Y. Macromolecules 2004;37:18.
[31] Gan LH, Ravi P, Mao BW, Tam KC. J Polym Sci, Part A: Polym Chem 2003;41:2688.
[32] Matyjaszewski K, Patten TE, Xia J. J Am Chem Soc 1997;119:674.
[33] Patrickios CS, Hertler WR, Abbott NL, Hatton HA. Macromolecules 1994;27:930.
[34] Akcasu Z, Han CC. Polymer 1981;22:1019.